

Article

The Role of Soil Salinization in Shaping the Spatio-Temporal Patterns of Soil Organic Carbon Stock

Wenli Zhang ^{1,2,3}, Wei Zhang ^{1,2,*}, Yubing Liu ^{4,5}, Jutao Zhang ⁶, Linshan Yang ⁶, Zengru Wang ^{4,5}, Zhongchao Mao ^{1,3}, Shi Qi ⁶, Chengqi Zhang ⁶, Zhenliang Yin ⁶

This file includes:

1. Supplementary Figures

Figures. S1 to S10

2. Supplementary Tables

Tables S1 to S3

1. Supplementary Figures

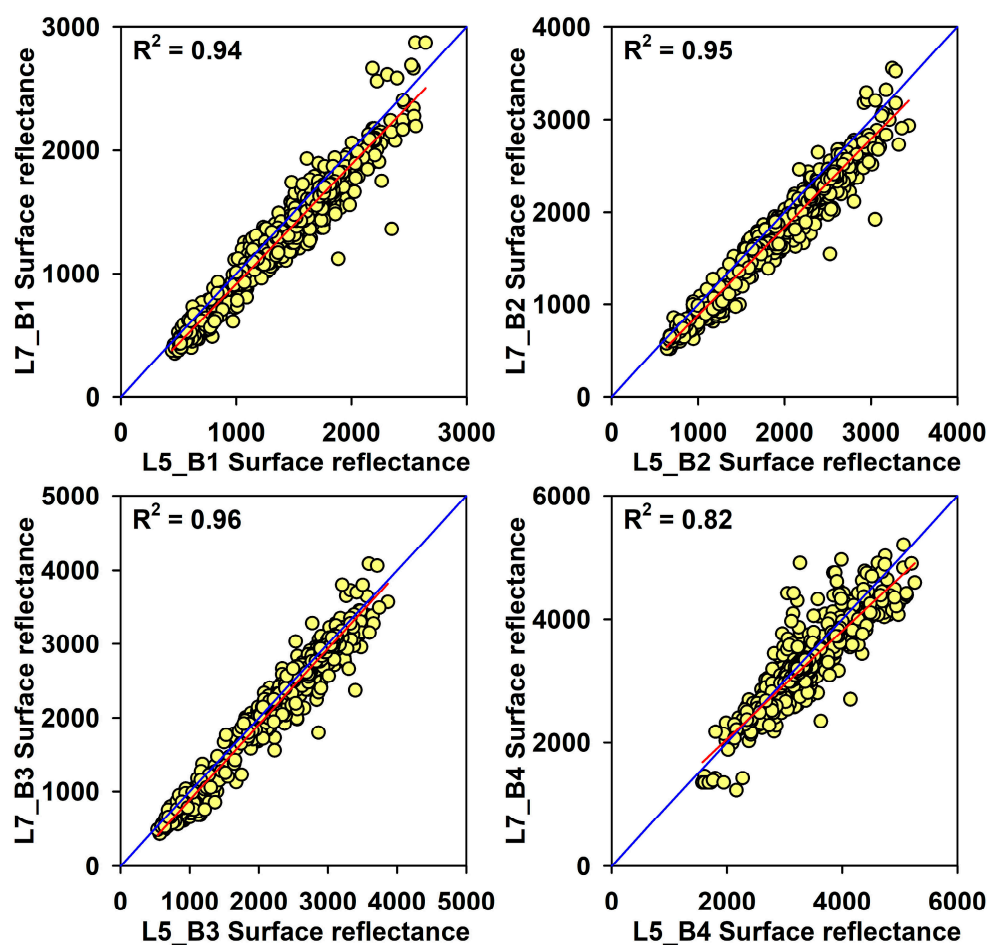


Figure S1. Relationships between the surface reflectance of Landsat 7 ETM+ and Landsat 5 TM for different bands. Note: For ETM+ and TM, the B1, B2, B3 and B4 represent the blue, green, red and near-infrared band, respectively.

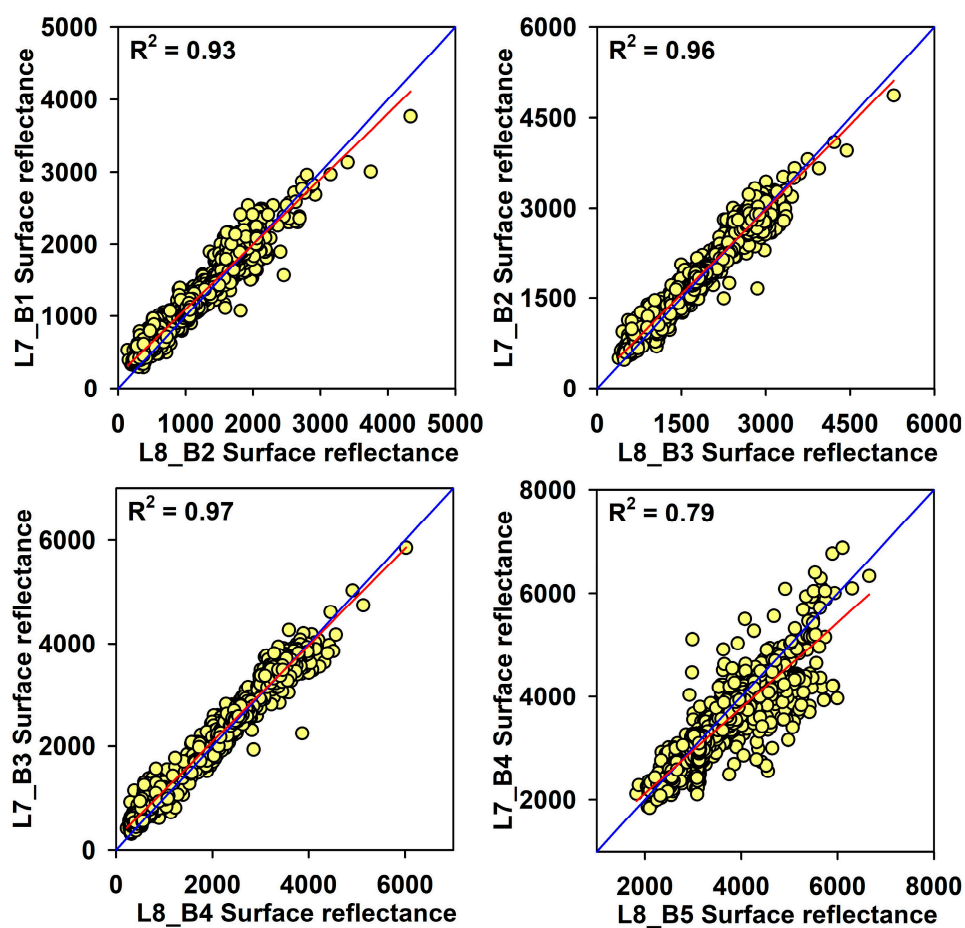


Figure S2. Relationships between the surface reflectance of Landsat 7 ETM+ and Landsat 8 OLI for different bands. Note: For OLI, the B2, B3, B4 and B5 represent the blue, green, red and near-infrared bands, respectively.

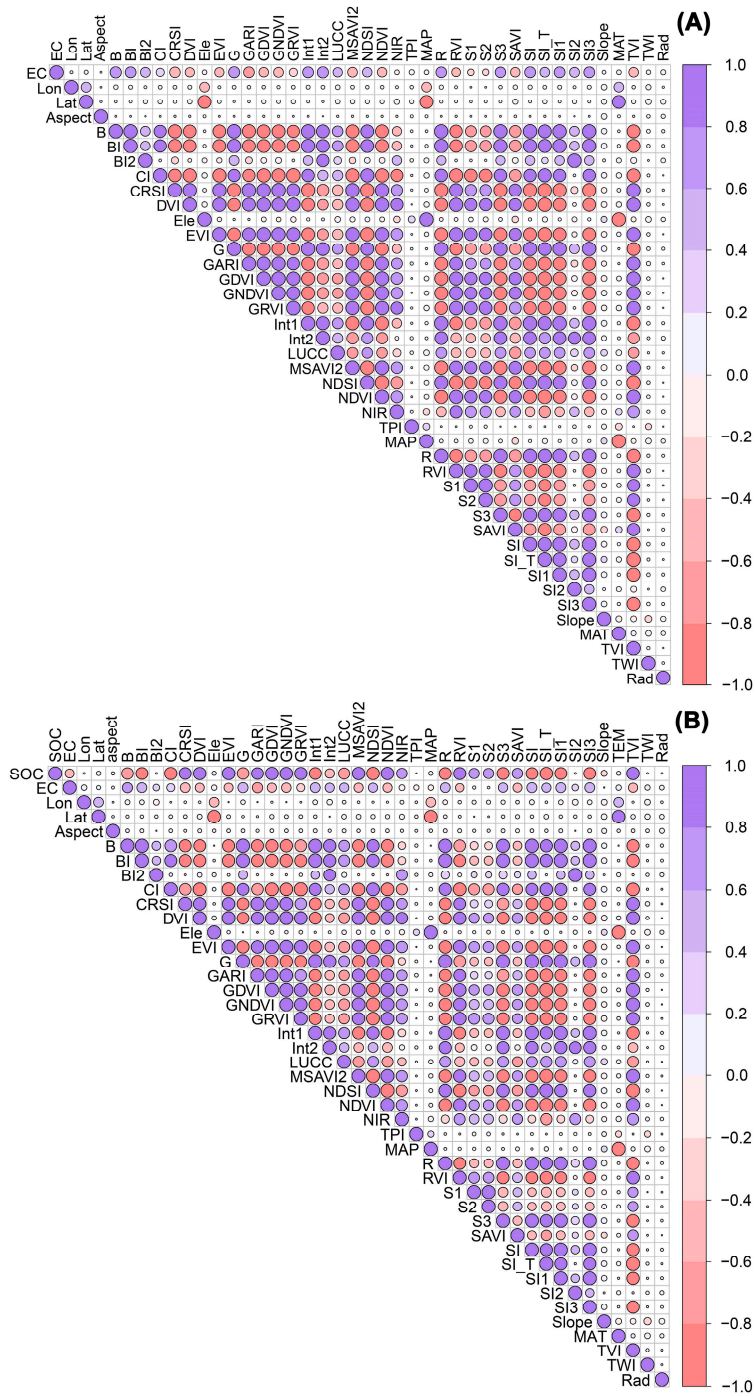


Figure S3. Correlation coefficients between site-level measurements and environmental covariates for soil EC (A) and SOC stock (B).

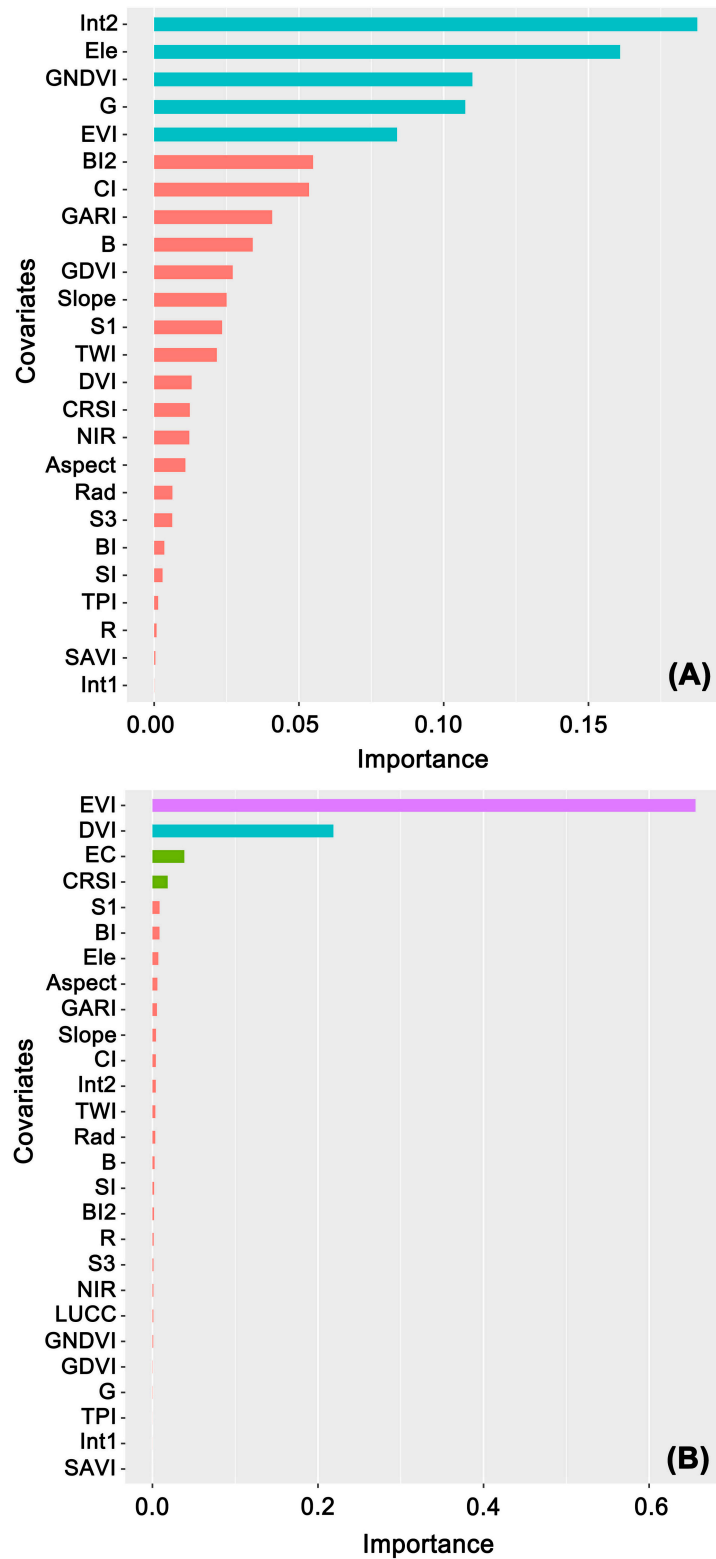


Figure S4. Variable importance of the covariates in modelling soil EC (A) and SOC stock (B) based on 30 times of the ten-fold cross-validation procedures.

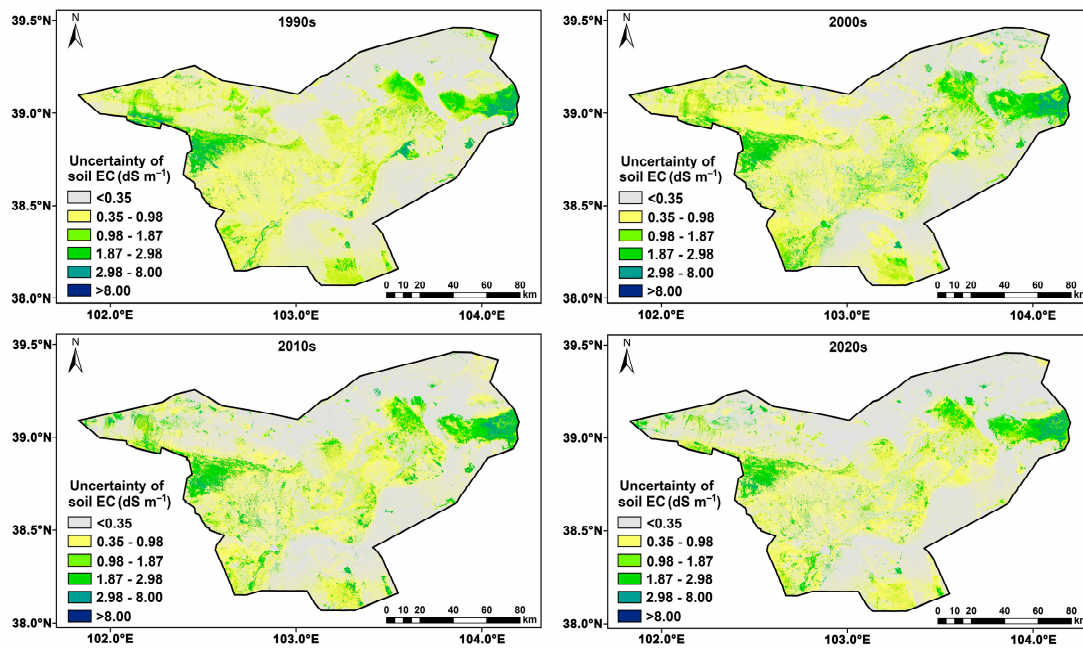


Figure S5. Spatial distribution maps of soil EC uncertainty derived from the XGBoost models for 1990s, 2000s, 2010s and 2020s. The uncertainty was expressed as standard deviation of the 30 bootstrap predictions.

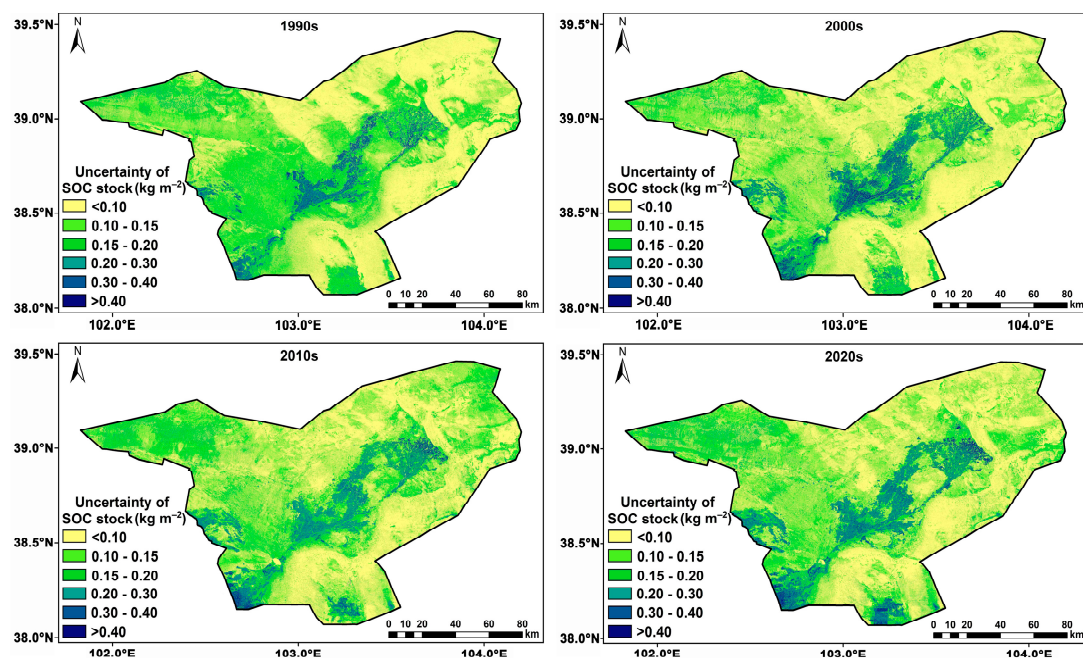


Figure S6. Spatial distribution maps of SOC stock uncertainty derived from the XGBoost models for 1990s, 2000s, 2010s and 2020s. The uncertainty was expressed as standard deviation of the 30 bootstrap predictions.

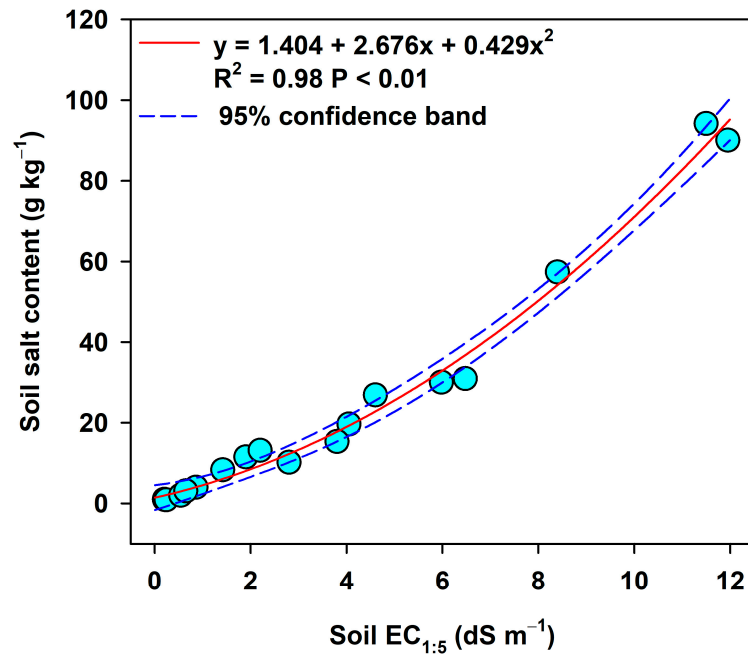


Figure S7. Relationships between soil salt content and soil $\text{EC}_{1:5}$ in the study area based on typical sampling site along the salinity gradient. Note: the soil salt content was obtained by summing up content of the eight main ions (Cl^- , SO_4^{2-} , CO_3^{2-} , HCO_3^- , Na^+ , Ca^{2+} , Mg^{2+} and K^+).

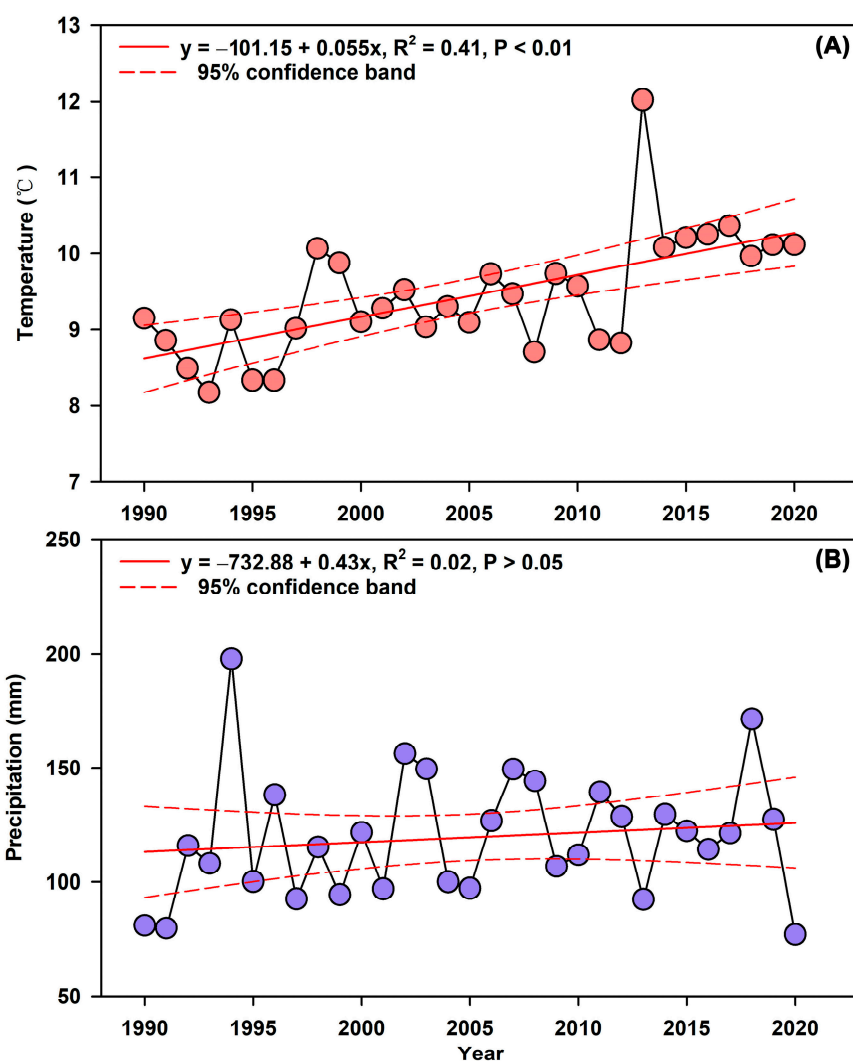


Figure S8. Temperature and precipitation changes during 1990–2020 based on the meteorological observation in Minqin station.

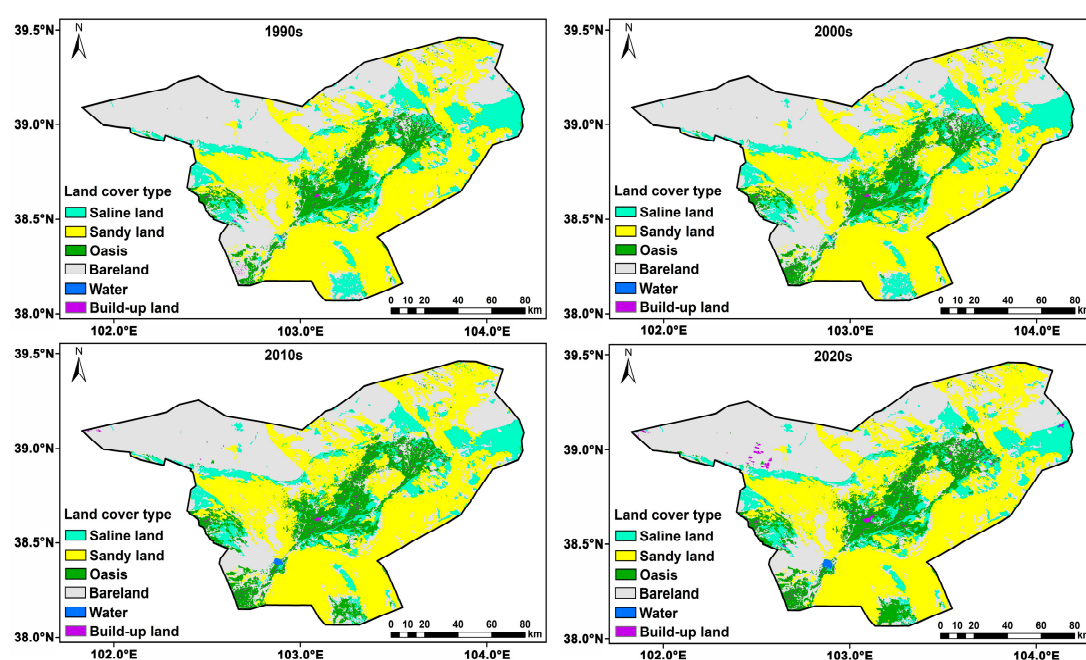


Figure S9. Land use and land cover changes from 1990s to 2020s.

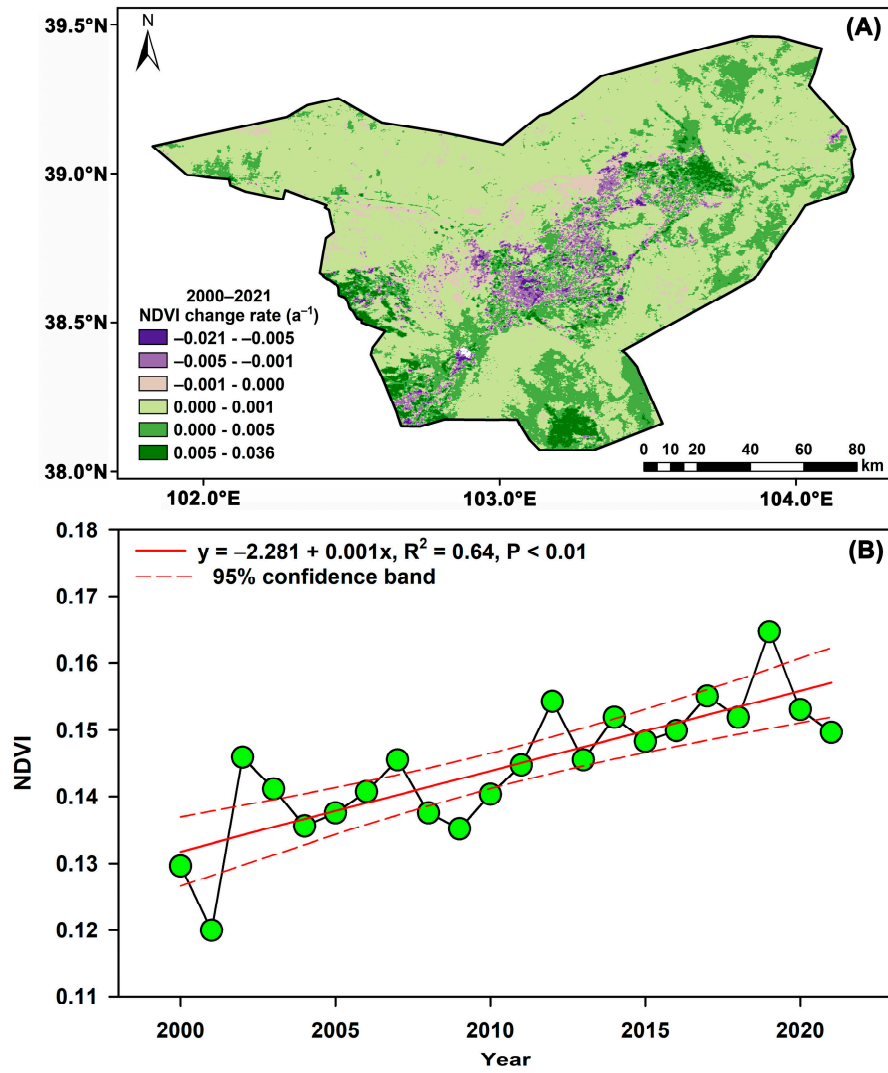


Figure S10. Spatial patterns of NDVI change rate (slope of the linear regression at each pixel) from 2000 to 2020 (A) and annual variation of area-weighted mean NDVI (B) based on the the MOD13Q1 NDVI datasets.

2. Supplementary Tables

Table S1. Environmental covariates used for soil mapping in this study.

Type	Predictor	Full name	Resolution (m)	Formula/Source
Vegetation index	NDVI	Normalized Differences Vegetation Index	30	$(\text{NIR}-\text{R})/(\text{NIR}+\text{R})$
	GNDVI	Green Normalized Difference Vegetation Index	30	$(\text{NIR}-\text{G})/(\text{NIR}+\text{G})$
	TVI	Transformed Vegetation Index	30	$100 * ((\text{NIR}-\text{R})/(\text{NIR}+\text{R})+0.5)^{0.5}$
	EVI	Enhanced Vegetation Index	30	$2.5 * (\text{NIR}-\text{R})/(\text{NIR}+6 * \text{R}-7.52 * \text{B}+1)$
	SAVI	Soil Adjusted Vegetation Index	30	$1.5 * (\text{NIR}-\text{R})/(\text{NIR}-\text{R}+0.5)$
	GRVI	Green-Red Vegetation Index	30	$(\text{G}-\text{R})/(\text{G}+\text{R})$
	RVI	Ratio Vegetation Index	30	NIR/R
	MSAVI2	Second Modified Soil Adjusted Vegetation Index	30	$(2 * \text{NIR}+1-\sqrt{(2 * \text{NIR}+1)^2-8 * (\text{NIR}-\text{R})})/2$
	DVI	Differences Vegetation Index	30	$\text{NIR}-\text{R}$
	GARI	Green Atmospherically Resistant Vegetation Index	30	$(\text{NIR}-(\text{G}+0.9 * (\text{B}-\text{R}))) / (\text{NIR}+(\text{G}+0.9 * (\text{B}-\text{R})))$
	CRSI	Canopy Response Salinity Index	30	$\sqrt{(\text{NIR} * \text{R}-\text{G} * \text{B}) / (\text{NIR} * \text{R}+\text{G} * \text{B})}$
	GDVI	Generalized Vegetation Index	30	$(\text{NIR}-\text{R})/(\text{NIR}+\text{R})$
Salt index	SI_T	Salinity Index	30	$100 * \text{R} / \text{NIR}$
	SI	Salinity index	30	$\sqrt{\text{B} * \text{R}}$
	NDSI	Normalized Differences salinity Index	30	$(\text{R}-\text{NIR})/(\text{R}+\text{NIR})$
	SI1	Salinity Index 1	30	$\sqrt{\text{G} * \text{R}}$
	SI2	Salinity Index 2	30	$\sqrt{\text{G} * \text{G}+\text{R} * \text{R}+\text{NIR} * \text{NIR}}$
	SI3	Salinity Index 3	30	$\sqrt{\text{G} * \text{G}+\text{R} * \text{R}}$
	S1	Salinity index I	30	B / R
	S2	Salinity index II	30	$(\text{B}-\text{R})/(\text{B}+\text{R})$
	S3	Salinity index III	30	$(\text{G} * \text{R}) / \text{B}$
	Int1	Intensity Index 1	30	$(\text{G}+\text{R})/2$
	Int2	Intensity Index 2	30	$(\text{G}+\text{R}+\text{NIR})/2$
Bright-related index	BI	Brightness Index	30	$(\sqrt{\text{R} * \text{R}+\text{G} * \text{G}})/2$
	BI2	The Second Brightness Index	30	$(\sqrt{\text{R} * \text{R}+\text{G} * \text{G}+\text{NIR} * \text{NIR}})/2$
	CI	Colour Index	30	$(\text{R}-\text{G})/(\text{R}+\text{G})$

Bands	B	Blue	30	Landsat images from GEE
	G	Green	30	Landsat images from GEE
	R	Red	30	Landsat images from GEE
	NIR	Near-infrared	30	Landsat images from GEE
Topographic index	Ele	Elevation	30	ASTER GDEM
	Slope	Slope	30	SAGA GIS
	Aspect	Aspect	30	SAGA GIS
	TWI	Topographic Wetness Index	30	SAGA GIS
	TPI	Multi-scale Topographic Position Index	30	SAGA GIS
	Rad	Potential Radiation	30	[53]
Climate	Tem	Temperature	1000	[54]
	Pre	Precipitation	1000	[54]
Human activity	LUCC	Land use and land cover change	30	http://www.resdc.cn
Locations	Lon	Longitude	30	Coverted from raster variable
	Lat	Latitude	30	Coverted from raster variable

Table S2. The regression equations between ETM+ and TM as well as OLI.

Bands	Landsat 7 v.s. Landsat 5	Landsat 7 v.s. Landsat 8
Blue	$ETM+ = -54.7172 + 0.9697 \cdot TM$	$ETM+ = 188.8301 + 0.9045 \cdot OLI$
Green	$ETM+ = -70.2301 + 0.9553 \cdot TM$	$ETM+ = 160.0372 + 0.9385 \cdot OLI$
Red	$ETM+ = -136.6724 + 1.0236 \cdot TM$	$ETM+ = 210.7848 + 0.9385 \cdot OLI$
Near-infrared	$ETM+ = 301.3540 + 0.8769 \cdot TM$	$ETM+ = 462.4669 + 0.8290 \cdot OLI$

Table S3. Changes in area of land cover types from 1990s to 2020s.

Type	Area (km ²)			
	1990s	2000s	2010s	2020s
Oasis	1497.01	1537.15	1859.92	1925.64
Sandy land	6545.89	6507.74	6448.32	6290.48
Saline land	2021.97	2000.20	1764.37	1733.87
Water	2.10	2.10	13.86	21.10
Construction land	66.24	79.59	85.11	118.78
Bare land	6093.29	6099.72	6054.92	6136.62